Summary of the 2018/2019 Asian Winter Monsoon

This report summarizes the characteristics of the surface climate and atmospheric/oceanographic considerations related to the Asian winter monsoon for 2018/2019.

Note: The Japanese 55-year Reanalysis (JRA-55; Kobayashi et al., 2015) atmospheric circulation data and COBE-SST (Ishii et al., 2005) sea surface temperature (SST) data were used for this investigation. NOAA Interpolated Outgoing Longwave Radiation (OLR) data (Liebmann and Smith 1996) provided online by the U.S. NOAA Earth System Research Laboratory (ESRL) at https://www.esrl.noaa.gov/psd/ was referenced to infer tropical convective activity. The base period for the normal is 1981 – 2010. The term "anomaly" as used in this report refers to deviation from the normal.

1. Surface climate conditions

Temperatures for December 2018 to February 2019 were generally above normal from the eastern part of East Asia to the southern part of South Asia, and were below normal in and around the northwestern part of East Asia (Figure 15). In particular, seasonal mean temperatures were extremely high from the Okinawa/Amami region of Japan to southern China and from the central part of Southeast Asia to the southern part of South Asia, and were extremely low from western Mongolia to northwestern China. Precipitation amounts during this period were above normal in and around southern and western parts of East Asia and the northwestern part of Southeast Asia, and were below normal in the northeastern part of East Asia (Figure 16). Drier-than-normal conditions in and around the Philippines and warmer-than-normal conditions in and around Southeast Asia, as seen in typical anomaly patterns of past El Niño events, were observed around February.

Figure 17 shows the extreme climate conditions observed between December 2018 and February 2019. In December, extremely high temperatures were seen from the Okinawa region of Japan to Southeast Asia, and extremely low temperatures were seen in the northwestern part of East Asia. Extremely high precipitation amounts were observed from western Japan to eastern China and from Myanmar to northwestern Sumatra. In January, extremely high temperatures were seen from northeastern China to the southern part of Central Siberia and from southern China to the central part of Southeast Asia. Extremely high precipitation amounts were observed from southern China to western Thailand, and extremely low precipitation amounts were observed from northern Japan to the southern Korean Peninsula. In February, extremely high temperatures were seen from the Ogasawara Islands of Japan to southern China and from the central part of Southeast Asia to the southern part of South Asia.

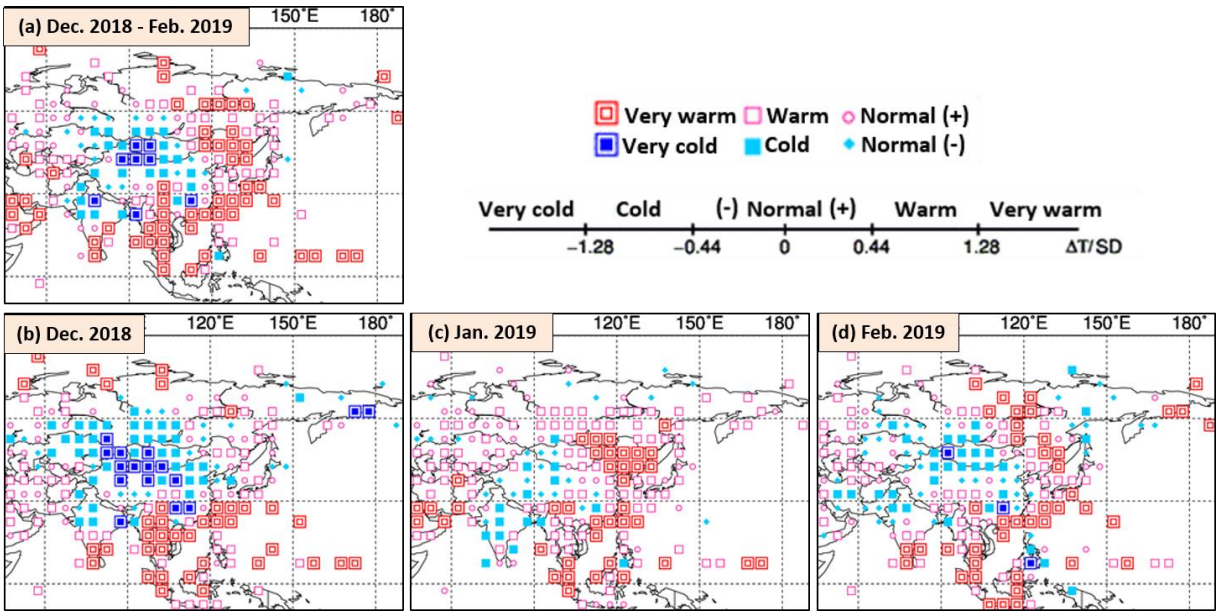

Figure 15 (a) Three-month mean temperature anomalies for December 2018 to February 2019, and monthly mean temperature anomalies for (b) December 2018, (c) January 2019 and (d) February 2019
Categories are defined by the three-month/monthly mean temperature anomaly against the normal divided by its standard deviation and averaged in 5° × 5° grid boxes. The thresholds of each category are -1.28, -0.44, 0, +0.44 and +1.28. Standard deviations were calculated from 1981 - 2010 statistics. Areas over land without graphical marks are those where observation data are insufficient or where normal data are unavailable.

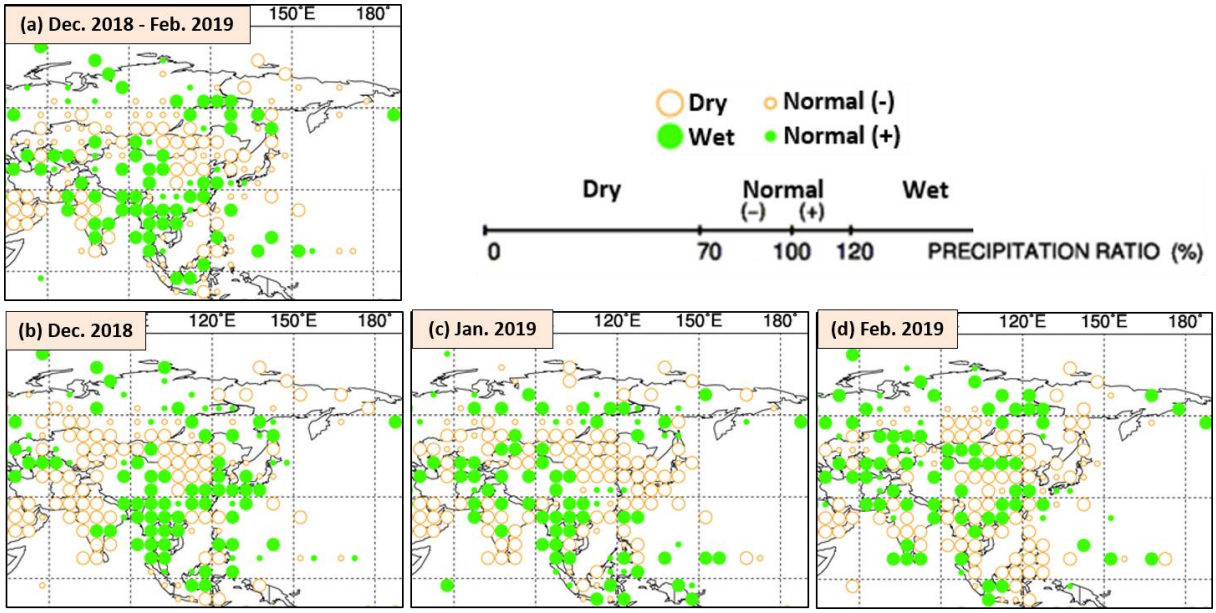

Figure 16 Three-month total precipitation ratio for December 2018 to February 2019, and monthly total precipitation ratio for (b) December 2018, (c) January 2019 and (d) February 2019

Categories are defined by the three-month mean precipitation ratio against the normal and averaged in 5° × 5° grid boxes. The thresholds of each category are 70, 100 and 120%. Areas over land without graphical marks are those where observation data are insufficient or where normal data are unavailable.

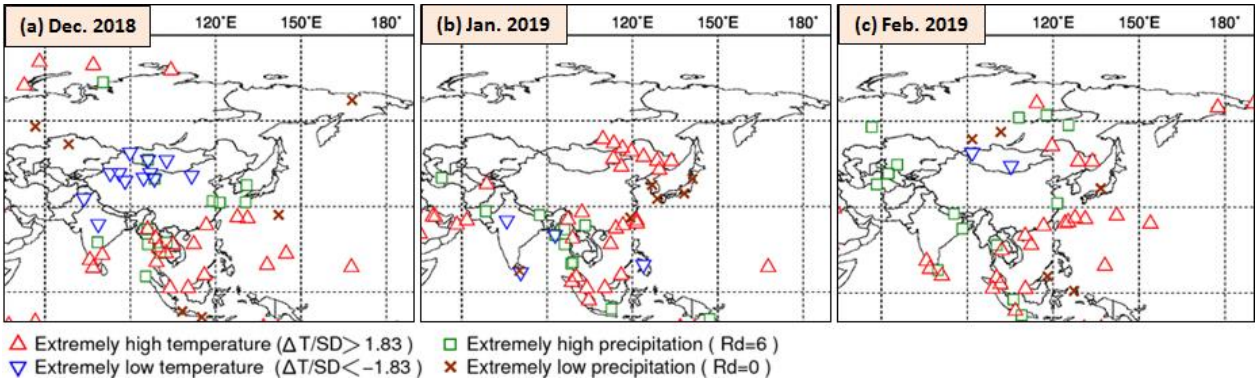

Figure 17 Extreme climate stations for (a) December 2018, (b) January 2019 and (c) February 2019

ΔT, SD and Rd indicate temperature anomaly, standard deviation and quintile, respectively.

2. Characteristic atmospheric circulation and oceanographic conditions

2.1 Conditions in the tropics

The El Niño conditions that developed in boreal autumn 2018 continued during winter 2018/2019. Positive SST anomalies were observed over almost the whole of the equatorial Pacific and in the equatorial Indian Ocean. In the North Pacific, remarkably positive SST anomalies were observed from the South China Sea to the central part (Figure 18).

Convective activity inferred from OLR during this period was enhanced to the west of the date line and suppressed from the southeastern tropical Indian Ocean to the Maritime Continent and around the Philippines (Figure 19). Over the Indochina Peninsula and the Malay Peninsula, where precipitation amounts during this period were above normal (Figure 16 (a)), convective activity was enhanced in December and January.

In the upper troposphere, large-scale divergent anomalies were seen over areas near the date line in association with enhanced convective activity, and convergent anomalies were observed over the Maritime Continent (Figure 20 (a)). In the 200-hPa stream function field, cyclonic circulation anomalies straddling the equator were seen over the Maritime Continent. A wave train was seen along the subtropical jet stream, with cyclonic circulation anomalies over northern India and anti-cyclonic circulation anomalies over the Middle East and the East China Sea (Figure 20 (b)). In the lower troposphere, cyclonic circulation anomalies straddling the equator were seen from west of the date line to the central Pacific, and anti-cyclonic circulation anomalies were seen around the Philippines (Figure 20 (c)).

The active phase of equatorial intraseasonal oscillation propagated eastward globally during winter 2018/2019 except in early February (Figure 21).

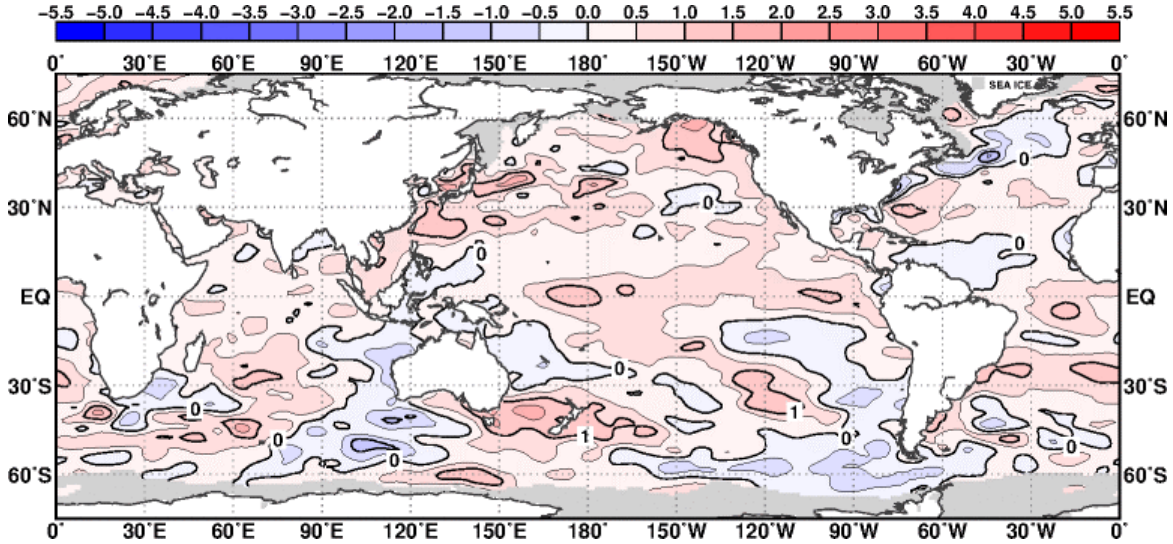

Figure 18 Three-month mean sea surface temperature (SST) anomalies [˚C] for December 2018 to February 2019
The contour interval is 0.5˚C.

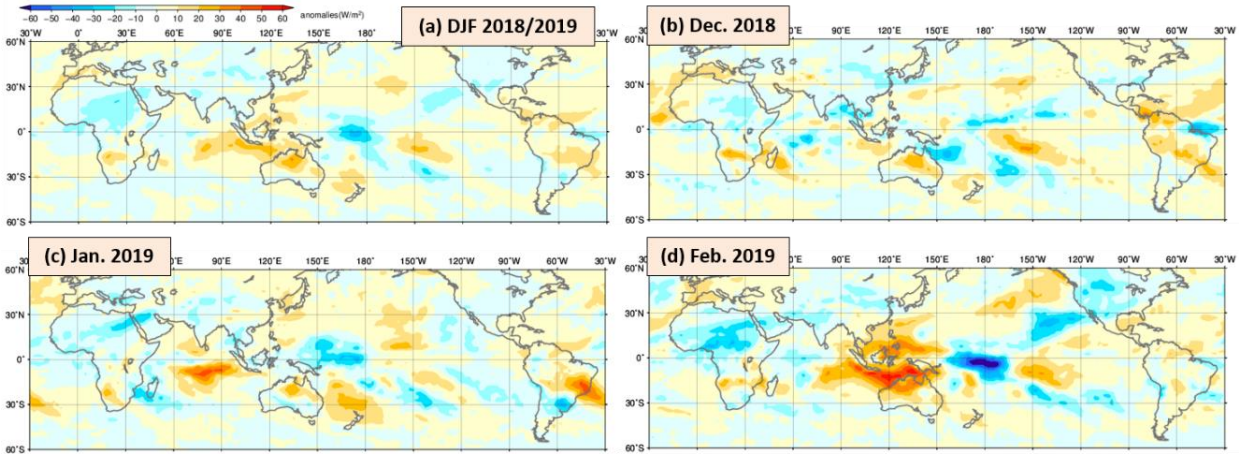

Figure 19 Outgoing longwave radiation (OLR) anomalies [W/m^2] (a) averaged over the three months from December 2018 to February 2019, for (b) December 2018, (c) January 2019 and (d) February 2019
The blue and red shading indicates areas of enhanced and suppressed convective activity, respectively.

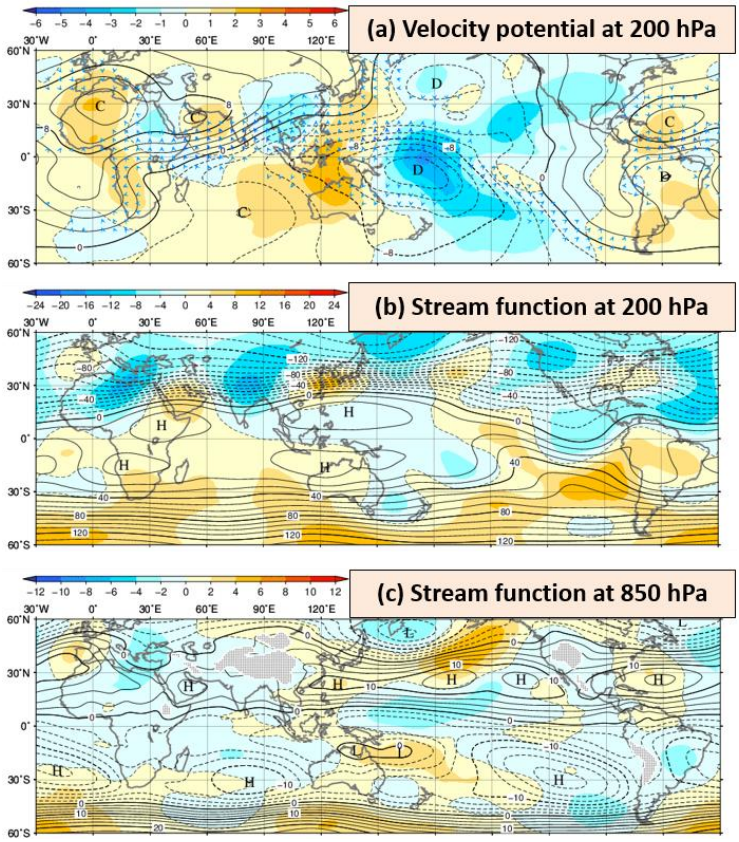

Figure 20 Three-month mean (a) 200-hPa velocity potential, (b) 200-hPa stream function, and (c) 850-hPa stream function for December 2018 to February 2019 [unit: 10^6 m^2/s]

(a) The contours indicate velocity potential at intervals of 2 × 10^6 m^2/s, and the shading shows velocity potential anomalies. D and C indicate the bottom and the peak of velocity potential, corresponding to the centers of large-scale divergence and convergence, respectively (b, c). The contours indicate stream function at intervals of (b) 10 and (c) 2.5 × 10^6 m^2/s, and the shading shows stream function anomalies. H and L denote the centers of anticyclonic and cyclonic circulations, respectively.

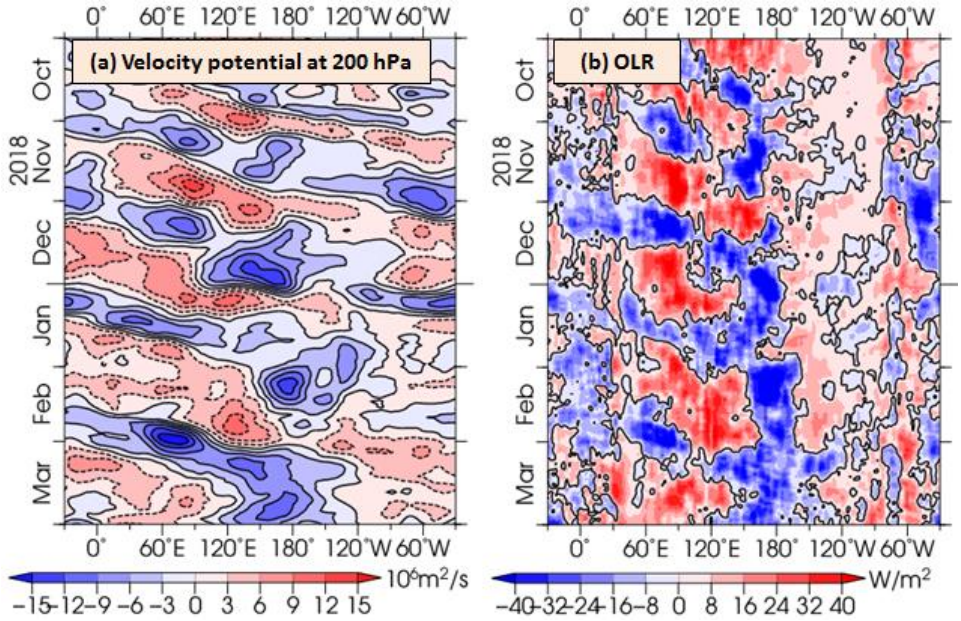

Figure 21 Time-longitude cross section of seven-day running mean (a) 200-hPa velocity potential anomalies [10^6 m^2/s] and (b) outgoing longwave radiation (OLR) anomalies [W/m^2] around the equator (5°S – 5°N) for October 2018 to March 2019

(a) The blue and red shading indicates areas of divergence and convergence anomalies, respectively. (b) The blue and red shading indicates areas of enhanced and suppressed convective activity, respectively.

2.2 Conditions in the extratropics

In the 500-hPa height field during winter 2018/2019, the polar vortex was centered near the North Pole and over the Kamchatka Peninsula. A wave train was seen over mid-latitudes with positive anomalies from eastern China to the seas east of Japan, and negative anomalies were seen from the western part of East Asia to the northern part of South Asia (Figure 22 (a)). Zonally elongated positive anomalies were seen from Japan to the area east of the country in December and February (Figure 22 (b), (d)).

The subtropical jet stream from North Africa to Eurasia meandered. The westerly jet stream shifted northward of its normal position from eastern China to Japan (Figure 23 (a)). Temperatures at 850 hPa (Figure 23 (b)) were above normal from southern China to the seas south of Japan, and were below normal over the northwestern part of East Asia.

In the sea level pressure field (Figure 24), negative anomalies were seen near the Kamchatka Peninsula throughout the period, indicating a northwestward shift of Aleutian Low activity. The Siberian High was stronger than normal over its normal position, and its eastward extension was weaker than normal. Positive anomalies were seen from Japan to the area east of the country in December and February.

(Hitoshi Sato, Tokyo Climate Center)

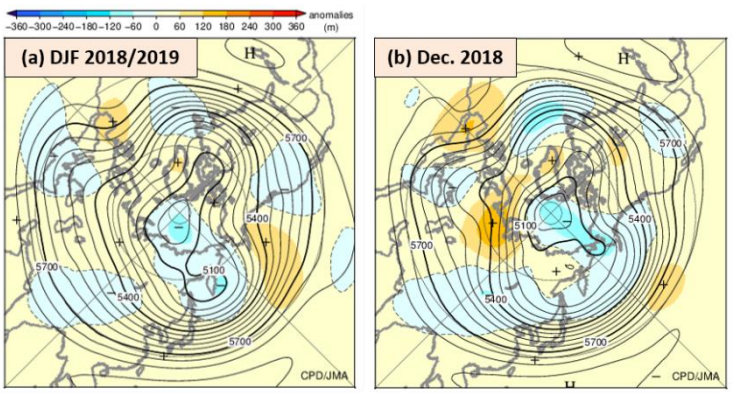

Figure 22 500-hPa height [m] (a) averaged over the three months from December 2018 to February 2019, for (b) December 2018, (c) January 2019 and (d) February 2019
The contours indicate 500-hPa height at intervals of 60 m, and the shading denotes anomalies. H and L indicate the peak and bottom of 500-hPa height, respectively, and + (plus) and – (minus) show the peak and bottom of anomalies, respectively.

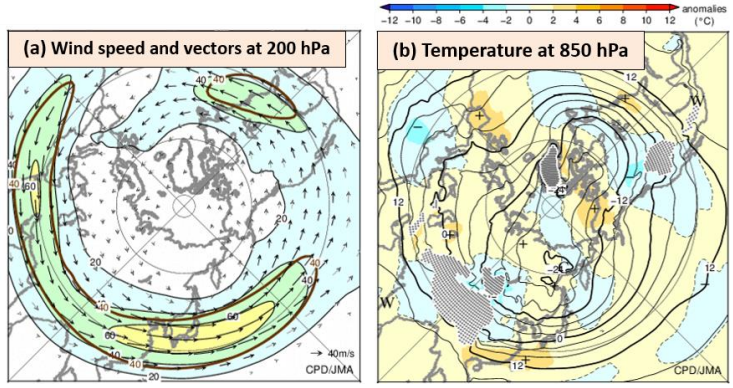

Figure 23 Three-month mean (a) 200-hPa wind speed and vectors [m/s] and (b) 850-hPa temperature [˚C] for December 2018 to February 2019
(a) The black lines show wind speed at intervals of 20 m/s, and the brown lines show its normal at intervals of 40 m/s. (b) The contours indicate 850-hPa temperature at intervals of 4 ˚C and the shading shows related anomalies.

References

Ishii, M., A. Shouji, S. Sugimoto and T. Matsumoto, 2005: Objective Analyses of Sea-Surface Temperature and Marine Meteorological Variables for the 20th Century using ICOADS and the Kobe Collection. *Int. J. Climatol.*, **25**, 865-879.

Kobayashi, S., Y. Ota, Y. Harada, A. Ebita, M. Moriya, H. Onoda, K. Onogi, H. Kamahori, C. Kobayashi, H. Endo, K. Miyaoka, and K. Takahashi, 2015: The JRA-55 Reanalysis: General Specifications and Basic Characteristics. *J. Meteorol. Soc. Japan*, **93**, 5 – 48.

Liebmann, B., and C. A. Smith, 1996: Description of a complete (interpolated) outgoing longwave radiation dataset. *Bull. Amer. Meteor. Soc.*, **77**, 1275–1277.

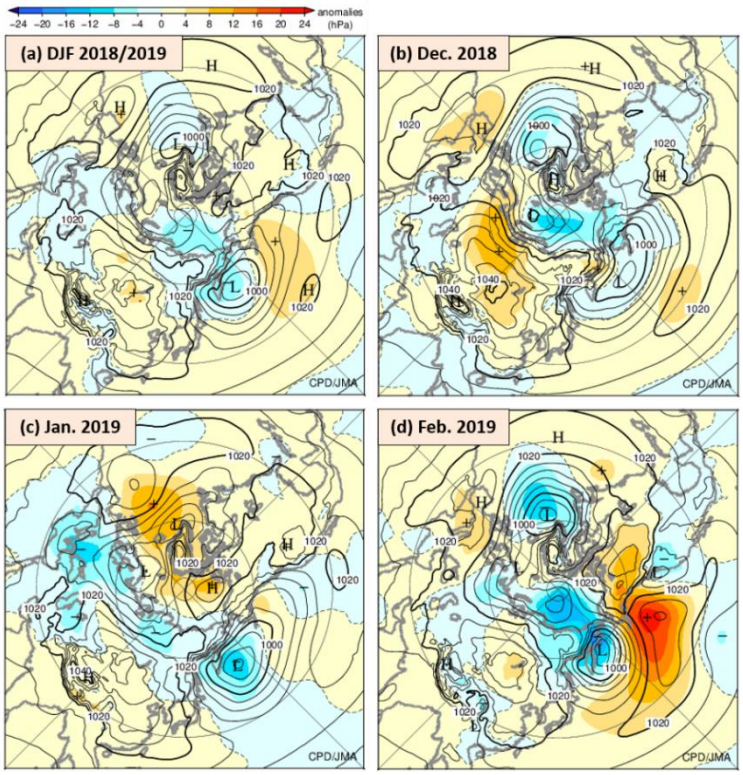

Figure 24 Sea level pressure [hPa] (a) averaged over the three months from December 2018 to February 2019, for (b) December 2018, (c) January 2019 and (d) February 2019
The contours indicate sea level pressure at intervals of 4 hPa, and the shading shows related anomalies. H and L indicate the centers of high and low pressure systems, respectively, and + (plus) and – (minus) show the peak and bottom of sea level pressure anomalies, respectively.

[<< Table of contents]